Hindawi Publishing Corporation
Journal of Chemistry
Volume 2015, Article ID 819580, 6 pages
http://dx.doi.org/10.1155/2015/819580

*Research Article*

# Effect of Graphene Nanosheets on the Morphology, Crystallinity, and Thermal and Electrical Properties of Super Tough Polyamide 6 Using SEBS Compounds

**Farzaneh Alirezaei Hoor,[1] Jalil Morshedian,[1] Shervin Ahmadi,[1] Mohammad Rakhshanfar,[1] and Alireza Bahramzadeh[2]**

[1]*Department of Polymer Processing, Iran Polymer and Petrochemical Institute, P.O. Box 14965/115, Tehran, Iran*
[2]*School of Chemical Engineering, College of Engineering, University of Tehran, P.O. Box 11155-4563, Tehran, Iran*

Correspondence should be addressed to Alireza Bahramzadeh; bahramzadeh@ut.ac.ir

Received 12 July 2015; Revised 26 September 2015; Accepted 5 October 2015

Academic Editor: Ewa Schab-Balcerzak



Super tough polyamide 6 was prepared by using SEBS and effect of SEBS-g-MA as a compatibilizer of PA6/SEBS matrix on mechanical properties was investigated. Thus super tough polyamide 6/graphene nanocomposites were produced using graphene nanosheets (GNs) through the melt compounding method. To compare the effectiveness of graphene, effects of graphite and carbon black (the other carbon structures) are also studied on the same matrix. The effects of graphene on crystallinity, improvements of morphology, and thermal and electrical properties of the nanocomposites were researched and compared with similar samples of graphite and carbon black. Due to the reaction between the maleic anhydride groups of SEBS and amine groups of nylon chains during the melt mixing process, super tough polyamide 6 was produced with high impact and tensile strength. The most important results of this study can be noted as an increase in the electrical conductivity and thermal stability by adding graphene to PA6/SEBS blend. Also the effect of graphene compatibility on PA6/SEBS/SEBS-g-MA blend was investigated with studying morphology.

## 1. Introduction

Due to the unique properties of graphene, a monolayer nanostructure of carbon atoms arranged in a honeycomb network, it has attracted a lot of attention nowadays. Graphene with unique properties of its nanostructure provides a large surface area as well as remarkable mechanical, electrical, and thermal properties and an effective optical property together with ultrahigh electron mobility [1, 2]. These incomparable properties make graphene appropriate for many applications, such as conducting electrically and thermally reinforced polymer composite, sensors, electronic circuits, flexible and transparent electrodes in screens, and solar cells [3]. Polymer/graphene nanocomposite is regarded as one of the major applications of graphene nanosheets (GNs). GNs have emerged as a glorious reinforcing nanocharge in polymer composites because of their unique thermal, electrical, and mechanical properties such as extremely high thermal conductivity (5,000 W/m K at 27°C), low resistivity (1026 Xcm), and very high mechanical strength and modulus (50 GPa) [4, 5].

Ding et al. Showed [6] improved thermal conductivity from 0.196 $W \cdot m^{-1} \cdot K^{-1}$ in neat polyamide to 0.416 $W \cdot m^{-1} \cdot K^{-1}$ in the thermal conductive polyamide 6/graphene composites (PG), which are produced by in situ polymerization of e-caprolactam and only 10 percent of Reduced Graphene Oxide (RGO) was used as filler. Zhang et al. prepared [1] PA6/GN composite by melt compounding and showed the good dispersion of graphene sheets in the polyamide matrix by using SEM. But no studies on the effect of graphene on super tough polyamide 6 with SEBS have been done so far.

PA6 as an interesting engineering polymer has extraordinary mechanical, thermal, and abrasion resistance properties; however, its low impact strength has declined the dimensional stability and application of PA6 [4, 7]. Rubber toughening is considered as an economical and effective method

Table 1: Formulation of the polyamide blends.

| Sample | PA6 % | SEBS % | SEBS-g-MA % |
|---|---|---|---|
| PA6 | 100 | 0 | 0 |
| M0 | 80 | 20 | 0 |
| M2 | 78 | 20 | 2 |
| M4 | 76 | 20 | 4 |
| M6 | 74 | 20 | 6 |
| M10 | 70 | 20 | 10 |

to toughen and extend applications of nylon without any significant increase in its price or decrease in its engineering properties [8–10].

In this study, a triblock elastomer, styrene ethylene/butylene-styrene (SEBS), and SEBS grafted with maleic anhydride (SEBS-g-MA) as an appropriate compatibilizer for PA6/SEBS blend were used. Consequently super tough polyamide 6 (PA6/SEBS/SEBS-g-MA) will be produced with high impact resistance. As noted above with regard to the advantages of using GNs, the development of a composite material based on GNs is of request. In this study, super tough PA6/graphene nanocomposites were prepared by melt mixing and crystallinity, electrical properties, and thermal stability were investigated.

## 2. Experimental

*2.1. Materials.* Raw materials used in this project include commercial polyamide 6 Akulon F-232 manufactured by DSM, SEBS triblock elastomer KRATON G165 (containing 13 wt.% styrene), and SEBS-g-MA compatibilizer KRATON FG1901X (containing 30% styrene and 1.8 percent maleic anhydride) supplied by Shell. Nanographene C60 made by Iran Nano-polymer Company, graphite 160-80N manufactured by GrafTech, and carbon black N330 from Iranian Pars Sazeh Company were used in order to prepare nanocomposites.

*2.2. Preparation of Super Tough Polyamide.* At first, polyamide 6 dried in an oven at 80°C for 24 h before use. The blends were prepared by thoroughly mixing PA6, SEBS, and MA-g-SEBS according to formulations in Table 1, followed by melt mixing in a twin screw extruder (BRABENDER) operating at 60 rpm and with extruder temperature profile of 210, 220, 230, 235, 230, and 235°C. The blends were quenched subsequently in water, pelletized into chips, and dried in a vacuum for 24 h at 80°C. The specimens for tests were produced using an ASLANIAN EM80 injection molding machine. In all the blends, weight percentages of SEBS were fixed in 20% by considering the practical issues and experiences of other researchers [11].

*2.3. Preparation of Super Tough Polyamide/Graphene Nanocomposites.* PA6/SEBS/SEBS-g-MA/graphene nanocomposites, based on formulation mentioned in Table 2, were prepared through melt mixing in the internal mixer at a setting temperature of 240°C, with a screw speed of 60 rpm, and then turned into sheets with standard thicknesses using a hot press (temperature 250°C, pressure 50 kg/cm$^2$ for 10 min). (Notably, 240°C was chosen in mixing step with respect to the same torque value of PA6 and SEBS at this temperature.)

*2.4. Characterization.* In order to study the microstructure morphology, scanning electron microscopy (Vega II XMU, Tescan, Czech Republic) was used. Notched Izod impact strength of the samples was measured following the procedures described in ISO180 at −40°C, using a 2.75 kg impact tester from Resil Impactor machine (Ceast Co., Italy). Tensile tests were carried out on an Instron 6025 (UK) machine at room temperature according to the ISO 527 test method at the speed of 50 mm/min. A minimum of five samples was tested in each series for determination of impact and tensile properties.

The thermal behavior of the samples was examined using differential scanning calorimeter (DSC) manufactured by Mettler Toledo, Switzerland. All samples were heated at temperature of 100°C up to 300°C with the speed of 10°C/min and under a nitrogen atmosphere. In order to investigate the thermal stability, the TGA machine model PL-1500 made by a British thermal science division was used. Heating rate of 10°C/min was performed from room temperature to 600°C under $N_2$ atmosphere. The determination of the surface electrical resistance was performed by resistance thermometers of the Rizpardazan Company of Iran, 4PP-R2K model, according to ASTM D257 standard. Moreover, X-ray diffraction (XRD) analysis was carried out over the 15°–30° angles, by X-ray diffraction Philips X'pert with the speed of 1/2 degrees/min.

## 3. Results and Discussion

Table 3 presents the results of mechanical properties of the samples that were studied by means of both tensile and impact tests. By increasing the MA (maleic anhydride) content up to 6%, modulus and tensile strength were decreased and impact strength and elongation at break were increased significantly. This is due to the reaction between the maleic anhydride groups of SEBS and amine groups of nylon chains during the melt mixing process, thereby making a link between SEBS and nylon [12]. This leads to transferring the mechanical tension between the two phases and increasing impact strength. Improvement of the interface between the two phases is responsible for prevention of adhesive failure; therefore failure occurs cohesively at higher strain. The best mechanical properties are obtained for the M6 sample which contains 6 wt.% SEBS-g-MA as a compatibilizer, and consequently super tough polyamide 6 was produced by using SEBS and SEBS-g-MA. However, this process has changed by adding more than 6 percent of the compatibilizer. It seems that adding more than this amount, to the constant concentration of SEBS, leads to formation of micelles by agglomeration of the compatibilizer molecules in other places besides the interface of matrix and dispersed phase, which consequently can decrease some of the properties.

SEM images of a PA6/SEBS/SEBS-g-MA mixture with/without the presence of graphene can be seen in Figure 1. Black holes in the pictures are related to the rubber phase

Table 2: Formulation of the nanocomposites samples.

| Sample | PA6 (%) | SEBS (%) | SEBS-g-MA (%) | Graphene (%) | Graphite (%) | Carbon black (%) |
|---|---|---|---|---|---|---|
| N1 | 74 | 20 | 6 | 1 | | |
| N3 | 74 | 20 | 6 | 3 | | |
| G1 | 74 | 20 | 6 | | 1 | |
| G3 | 74 | 20 | 6 | | 3 | |
| CB1 | 74 | 20 | 6 | | | 1 |
| CB3 | 74 | 20 | 6 | | | 3 |

Table 3: Mechanical properties of samples.

| Sample | Impact strength (kJ/m$^2$) | Elongation at break (%) | Tensile strength (MPa) | Modulus (MPa) |
|---|---|---|---|---|
| PA6 | 4.26 ± 0.4 | 60.3 ± 1.6 | 64.3 ± 3 | 1208.6 ± 21.7 |
| M0 | 4.9 ± 0.2 | 70.7 ± 3 | 44.9 ± 0.8 | 939.3 ± 4.4 |
| M2 | 11.13 ± 0.6 | 145.3 ± 8.4 | 36.1 ± 3 | 858.5 ± 17.4 |
| M4 | 13.71 ± 0.6 | 179.6 ± 3 | 36.2 ± 0.6 | 830 ± 14.5 |
| M6 | 14.96 ± 0.5 | 224 ± 1.6 | 37.9 ± 0.3 | 901 ± 4.1 |
| M10 | 13.5 ± 0.9 | 148.3 ± 9.9 | 38.7 ± 2.9 | 797 ± 14 |

and are extracted by boiling xylene. In the M6 sample, size of the dispersed phase is about 1 micrometer. However, the addition of graphene has changed the dispersed phase size to smaller dimensions in the nanometer range. It seems that the reduction of the dispersed phase size is due to increased viscosity of the PA6 matrix, due to the fact that, with an increase in the viscosity of matrix, dispersed phase viscosity ratio to the matrix decreases. Therefore, the viscous forces have become stronger and SEBS particles have undergone further deformation and their failure occurs more easily. Thus, the diameter of the dispersed phase droplets that were prepared by melt mixing will be smaller. Increasing the viscosity of the matrix can be used alone as a factor to reduce the particle size. But in addition to these factors, graphene sheets can act as a physical barrier and prevent coalescence of the dispersed phase droplets. As a result, they lead to a change in the morphology of the polymer alloy, which leads to a further reduction in the size of the dispersed phase [13]. So, it can be argued that graphene in PA6/SEBS blend acts as a compatibilizer. This behavior for nanoclay in different mixture has also been observed in the work of previous researchers [13, 14].

The peaks of $\alpha 1$ and $\alpha 2$ crystalline form of PA6 with high intensity and the peak of the $\gamma$-type crystals with lower intensity for all samples are seen in Figure 2 which shows the XRD patterns of different samples. However the area under the peak which represents the crystallization degree is different.

Table 4 shows the crystallinity of each sample using the area under XRD curve peak. By adding 1% graphene to PA6/SEBS/SEBS-g-MA matrix (N1), crystallinity decreased from 31.5% to 26.9%. This reduction continued with increasing graphene content up to 3% (N3). This process has been observed in the works of other researchers on pure polyamide [1, 6]. Graphene sheets with high aspect ratio (surface area to thickness) easily penetrate through polyamide chains and cause interruption in crystallization process. In addition, according to the SEM images it can be concluded that the graphene sheets interact with matrix and can act as physical barriers [13] and could interrupt the formation of crystals.

Table 4: Degree of nanocomposite crystallinity by calculating the area under the peak of XRD curve.

| Sample | Crystallinity (%) |
|---|---|
| M6 | 31.5 |
| N1 | 26.9 |
| N3 | 23.4 |
| G1 | 28.7 |
| G3 | 30.9 |
| CB1 | 31.6 |
| CB3 | 31.9 |

On the other hand, graphite acted differently. Low amount of graphite (G1) reduced the crystallinity more than the larger quantities. It is because of agglomeration of graphite sheets in higher amount (G3) due to their high surface energy which led to retention of sheets and a slight decrease in crystallinity. In lower quantities, graphite sheets had better possibility of dispersion in the matrix and acted as a physical barrier and finally reduced the crystallinity. G1 sample has lower crystallinity (28.7%) than G3 (30.9%) and M6 (31.5%) while the G3 sample has almost identical crystallinity to the sample without graphite (M6). Generally, graphite sheets have no significant effect in crystallinity process because their sheets are big and thick. Also, the crystallinity of CB1 (31.6%) and CB3 (31.9%) samples does not differ with M6 sample. This is because of the large and tightly packed clusters of carbon black that had no effect on the crystallization of polyamide.

The curves resulting from DSC test for M6 and N3 samples are presented in Figure 3. Both samples have a large peak at 221°C, showing the melting temperature of the compounds. In Table 5, the melting temperature ($T_m$), the

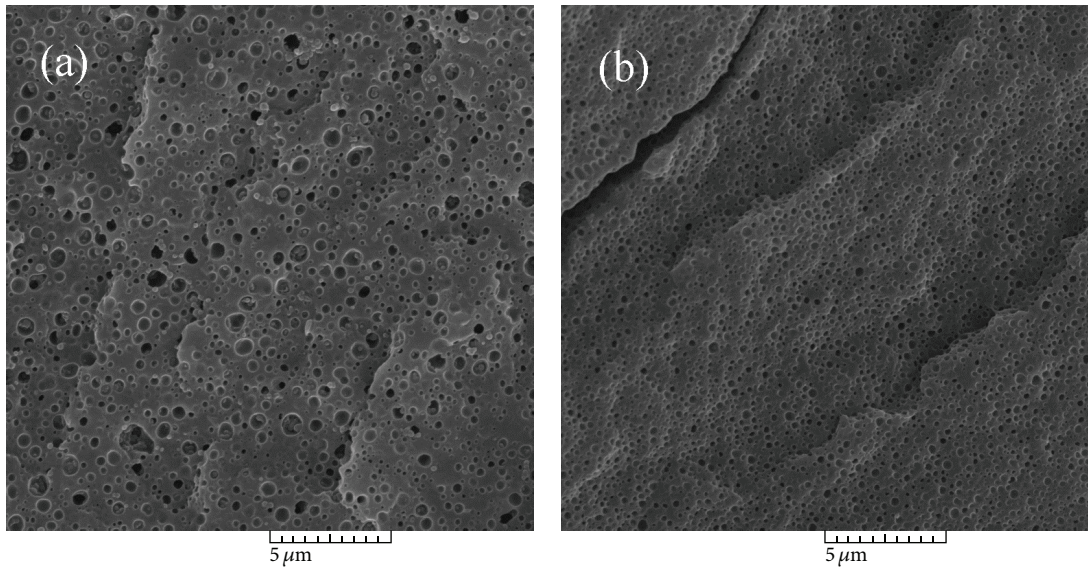


Figure 1: SEM images of the fracture surface of (a) M6 sample and (b) N1 sample.

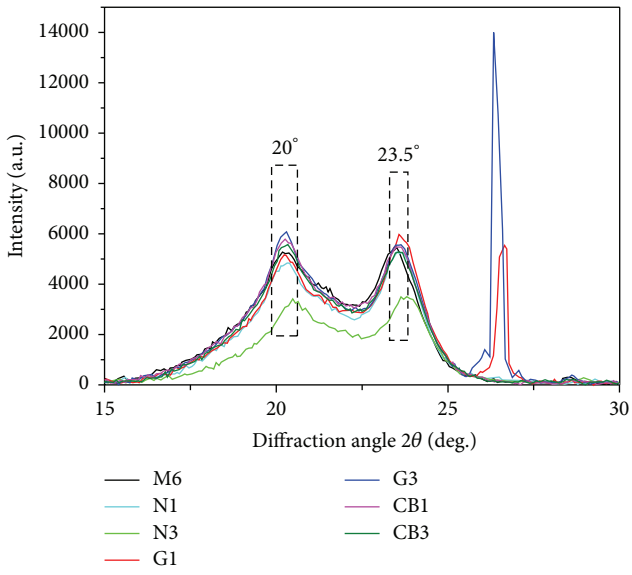


Figure 2: Wide-angle XRD diagram of nanocomposites.

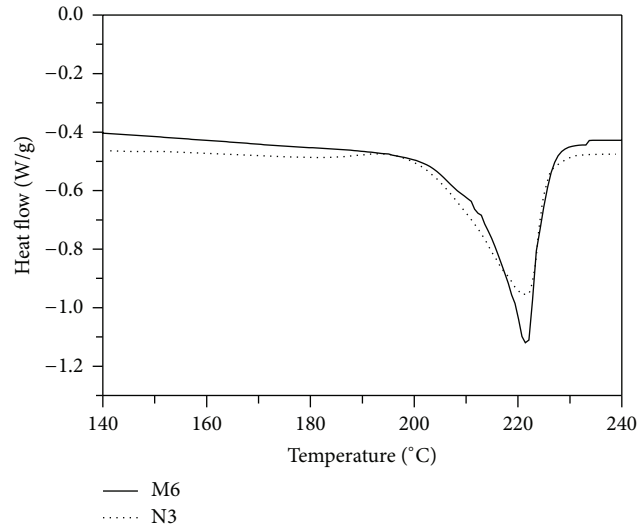


Figure 3: DSC melting curves of the M6% and N3% samples.

enthalpy of fusion ($\Delta H_f$), and the percentage of crystallinity ($\chi_c$) of the samples are shown. Crystallinity percentages were calculated using

$$\chi_c = \frac{\Delta H_f}{\Delta H_f^\circ * w_c}, \quad (1)$$

where ($\Delta H_f^\circ$) is the heat of fusion of 100% crystalline (PA6: $\Delta H_f^\circ = 230$) sample, $w_c$ is the weight percent of PA6 in the mixture, $\Delta H_f$ is the heat of fusion, and $\chi_c$ is the crystallinity percent of the sample [15, 16]. In comparison between M6 and N3 samples, a reduction in crystallinity of the N3 sample is observable. As noted above, it seems that small thickness of graphene has led to easy penetration in the polyamide chains. Graphene acts as a physical barrier due to its large surface area and causes interference in the crystallization process of polyamide [13]. Decrease in crystallinity of N3 sample which contains 3 wt.% graphene corresponds to the results of XRD analysis.

Table 5: Results of M6% and N3% sample heat map.

| Sample | $T_m$ (°C) | $\Delta H_f$ (J/g) | $\chi_c$ (%) |
|---|---|---|---|
| M6 | 221.4 | 54.71 | 32.14 |
| N3 | 221.3 | 47.77 | 28.06 |

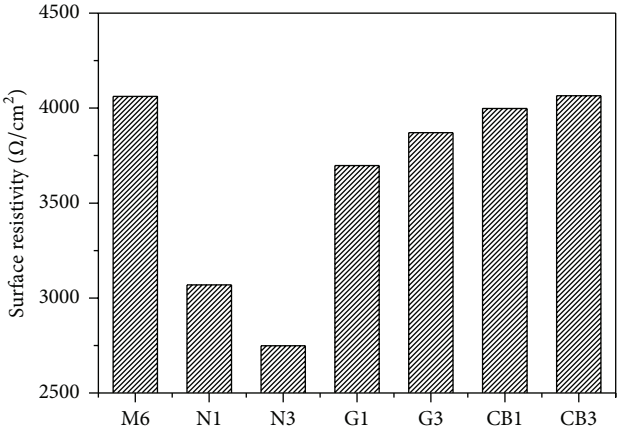


Figure 4: Electrical resistance of nanocomposites at 0.566 mA current intensity.

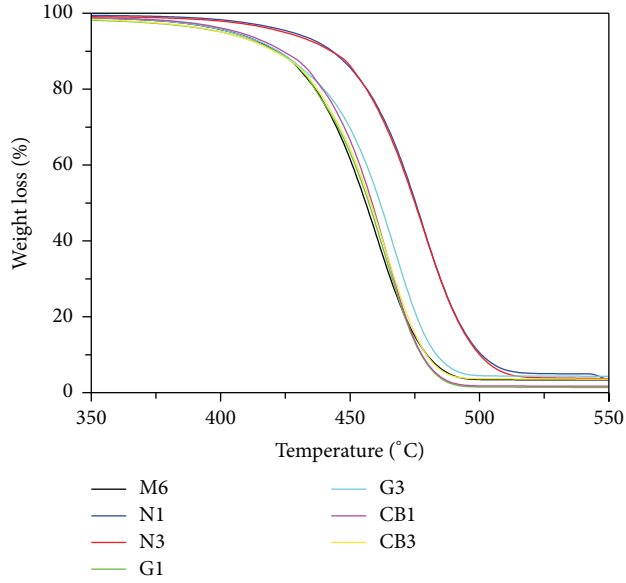


Figure 5: TGA curves of nanocomposites.

To investigate the electrical properties of the samples, the surface electrical resistivity factor was measured and the results can be seen in Figure 4. The electrical resistance of N3 sample is lower than other samples. This manifests the higher electrical conductivity of N3. According to the results of XRD and DSC, crystallinity of this sample has decreased. By reduction in crystallinity, dispersion of graphene sheets can be done better in the matrix [17]. Better dispersion of nanoparticles in the matrix with the morphology and intrinsic properties of graphene has increased the electrical conductivity. Thus, the N3, N1, and G1 samples which, respectively, have lower crystallinity than the rest of the samples contain less electrical resistance and consequently a higher electrical conductivity. Moreover placing graphene sheets together improves electron conduction paths and this is similar to the results of previous research on the use of graphene oxide [18].

To determine the samples thermal stability, TGA tests were performed. As it can be seen in Figure 5, the destruction of the N1 and N3 samples lasts longer and occurs at higher temperatures. These results demonstrated that the thermal stability of the sample by adding graphene has increased, compared to the neat and other samples. This is due to the presence of graphene particles with large surface area that act as barrier and a thermal insulation [1]. The TGA results are similar to previous researches [1, 6, 19] However, we observed higher degradation temperature and thermal stability in samples with graphite and carbon black compared to M6 sample due to the intensifying effect of these fillers, but the difference is negligible.

## 4. Conclusions

In this study, super tough polyamide 6 was produced by using SEBS and SEBS-g-MA, and its mechanical properties were investigated. Results of impact and tensile tests showed that the addition of 6% of SEBS-g-MA as a compatibilizer in PA6/SEBS (74/20) blend could provide appropriate mechanical properties. Therefore the effect of graphene on PA6/SEBS/SEBS-g-MA with 6% of compatibilizer was studied. By investigating the morphology of blends, it can be argued that the graphene can act as a compatibilizer for PA6/SEBS/SEBS-g-MA blend. DSC and XRD analysis results showed that the presence of nanometer graphene sheets interferes with the crystallization process and crystallinity decreases by about 25%. Also, with the addition of only 3 percent of graphene, we observed a sharp decrease in the surface electrical resistance and a sharp increase in thermal stability for samples with graphene. It is in the way that graphite and carbon black had no significant effect on these properties.

## Conflict of Interests

The authors declare that there is no conflict of interests regarding the publication of this paper.

## References

[1] P. P. Zhang, K. Y. Zhu, L. Q. Su, and R. Xiao, "Preparation and properties of graphene/polyamide 6 composites by melt compounding," in *Advanced Materials Research*, pp. 31–34, Trans Tech Publications, 2013.

[2] Y. Zhu, S. Murali, W. Cai et al., "Graphene and graphene oxide: synthesis, properties, and applications," *Advanced Materials*, vol. 22, no. 35, pp. 3906–3924, 2010.

[3] M. J. Allen, V. C. Tung, and R. B. Kaner, "Honeycomb carbon: a review of graphene," *Chemical Reviews*, vol. 110, no. 1, pp. 132–145, 2010.

[4] R. Bouhfid, F. Z. Arrakhiz, and A. Qaiss, "Effect of graphene nanosheets on the mechanical, electrical, and rheological properties of polyamide 6/acrylonitrile–butadiene–styrene blends," *Polymer Composites*, 2014.

[5] S. Basu and P. Bhattacharyya, "Recent developments on graphene and graphene oxide based solid state gas sensors," *Sensors and Actuators B: Chemical*, vol. 173, pp. 1–21, 2012.

[6] P. Ding, S. Su, N. Song, S. Tang, Y. Liu, and L. Shi, "Highly thermal conductive composites with polyamide-6 covalently-grafted graphene by an in situ polymerization and thermal reduction process," *Carbon*, vol. 66, pp. 576–584, 2014.

[7] X.-Q. Liu, W. Yang, B.-H. Xie, and M.-B. Yang, "Influence of multiwall carbon nanotubes on the morphology, melting, crystallization and mechanical properties of polyamide 6/acrylonitrile-butadiene-styrene blends," *Materials & Design*, vol. 34, pp. 355–362, 2012.

[8] L.-F. Ma, X.-F. Wei, Q. Zhang et al., "Toughening of polyamide 6 with $\beta$-nucleated thermoplastic vulcanizates based on polypropylene/ethylene-propylene-diene rubber grafted with maleic anhydride blends," *Materials and Design*, vol. 33, no. 1, pp. 104–110, 2012.

[9] Z. Liu, Y. Deng, Y. Han et al., "Toughening of polyamide-6 with a maleic anhydride functionalized acrylonitrile-styrene-butyl acrylate copolymer," *Industrial & Engineering Chemistry Research*, vol. 51, no. 27, pp. 9235–9240, 2012.

[10] C.-J. Wu, J.-F. Kuo, and C.-Y. Chen, "The role of the compatibilizer on morphologies and mechanical properties of polyamide 6/(styrene–[ethylene–butylene]–styrene) triblock copolymer blends," *Advances in Polymer Technology*, vol. 14, no. 2, pp. 129–136, 1995.

[11] E. Hajizadeh and H. Garmabi, "Response surface based optimization of toughness of hybrid polyamide 6 nanocomposites," *International Journal of Chemical & Biomolecular Engineering*, vol. 1, no. 1, pp. 40–44, 2008.

[12] M. I. Kohan, *Nylon Plastics Handbook*, vol. 378, Hanser, Munich, Germany, 1995.

[13] B. B. Khatua, D. J. Lee, H. Y. Kim, and J. K. Kim, "Effect of organoclay platelets on morphology of Nylon-6 and poly(ethylene-ran-propylene) rubber blends," *Macromolecules*, vol. 37, no. 7, pp. 2454–2459, 2004.

[14] Y. Li and H. Shimizu, "Novel morphologies of poly(phenylene oxide) (PPO)/polyamide 6 (PA6) blend nanocomposites," *Polymer*, vol. 45, no. 22, pp. 7381–7388, 2004.

[15] L. A. Utracki and C. A. Wilkie, *Polymer Blends Handbook*, Springer, Dordrecht, The Netherlands, 2014.

[16] J. E. Mark, *Polymer Data Handbook*, Oxford University Press, 2009.

[17] S. C. Tjong, G. D. Liang, and S. P. Bao, "Effects of crystallization on dispersion of carbon nanofibers and electrical properties of polymer nanocomposites," *Polymer Engineering and Science*, vol. 48, no. 1, pp. 177–183, 2008.

[18] H. R. Pant, B. Pant, C. H. Park et al., "RGO/Nylon-6 composite mat with unique structural features and electrical properties obtained from electrospinning and hydrothermal process," *Fibers and Polymers*, vol. 14, no. 6, pp. 970–975, 2013.

[19] H. Liu, L. Hou, W. Peng, Q. Zhang, and X. Zhang, "Fabrication and characterization of polyamide 6-functionalized graphene nanocomposite fiber," *Journal of Materials Science*, vol. 47, no. 23, pp. 8052–8060, 2012.